Room evacuation through two contiguous exits

I.M. Sticco[a], G.A. Frank[c], S. Cerrotta[a], C.O. Dorso[a,b]

[a] *Departamento de Física, Facultad de Ciencias Exactas y Naturales, Universidad de Buenos Aires, Pabellón I, Ciudad Universitaria, 1428 Buenos Aires, Argentina.*
[b] *Instituto de Física de Buenos Aires, Pabellón I, Ciudad Universitaria, 1428 Buenos Aires, Argentina.*
[c] *Unidad de Investigación y Desarrollo de las Ingenierías, Universidad Tecnológica Nacional, Facultad Regional Buenos Aires, Av. Medrano 951, 1179 Buenos Aires, Argentina.*

Abstract

Current regulations demand that at least two exits should be available for a safe evacuation during a panic situation. The second exit is expected to reduce the overall clogging, and consequently, improve the evacuation time. However, rooms having contiguous doors not always reduce the leaving time as expected. We investigated the relation between the door's separation and the evacuation performance. We found that there exists a separation distance range that does not really improve the evacuation time, or it can even worsen the process performance. To our knowledge, no attention has been given to this issue in the literature. This work reports how the pedestrian's dynamics differ when the separation distance between two exit doors changes and how this affects the overall performance.

Keywords:
Panic evacuation, Social force model, Clogging delay
PACS: 45.70.Vn, 89.65.Lm

1. Introduction

The practice of providing two doors for emergency evacuation can be traced back to the last Qing dynasty in China (1644-1911 AD). A mandatory regulation established that large buildings had to provide two fire exits [1]. This kind of regulations upgraded to current standard codes with detailed specifications on the exits position, widths and separations [2, 3].

Current regulations claim that the minimum door width should be 0.813 m while the maximum door-leaf should not exceed 1.219 m [3, 4]. If more than two doors are required, the distance between two of them must be at least one-half or one-third of the room diagonal distance. But, no special requirements apply to the rest of the doors.

The rulings leave some space for placing the extra openings (*i.e.* those above two exits) at an arbitrary separation distance. Thus, it is possible to place a couple of doors on the same side of the room at any distance. The special case of two contiguous doors has been examined throughout the literature [5, 6, 7, 8].

Kirchner and Schadschneider studied the pedestrians evacuation process through two contiguous doors using a cellular automaton model [5]. The agents were able to leave the room under increasing panic situations for behavioural patterns varying from individualistic pedestrians to strongly coupled pedestrians moving like a *herd*. The evacuation time was found to be independent of the separation distance between doors for the individualistic pedestrians in a panic situation. But if the pedestrians were allowed to move like a herd, an increasing evacuation time for small separation lengths (less than 10 individuals size) was reported.

The above conclusions are not in complete agreement with the investigation acknowledged in Ref. [6]. The authors assert that the total number of pedestrians leaving the room per unit time slows-down for separation distances (between doors) smaller than four door widths [6]. This slow-down is identified as a disruptive interference effect due to pedestrians crossing in each other's path. For the particular case analyzed in this work, the threshold of four door widths ($4\,d_w$) corresponds to the distance separation necessary to distinguish two independent groups of pedestrians, each one surrounding the nearest door.

Researchers called the attention on the fact that no matter how separated the two contiguous doors are placed, the overall performance does not improve twice with respect to a single exit (of the same total width). This effect is attributed to some sort of pedestrian interference [6].

Although the above results were obtained for very narrow doors (*i.e.* sin-

gle individual width), further investigation showed that they also apply to doors allowing two simultaneous leaving pedestrians. However, this does not hold for a room with a single door [7]. In this case, it is true that the mean flux of evacuating people increases with an increasing door width, but the ratio flux per door width decreases [9].

It was observed in Ref. [5, 7] that the two contiguous doors should not be placed near the wall corners, since the side walls affect negatively the evacuation efficiency. No further explanation was given on this phenomenon, although the authors concluded this may cause a worsening in the evacuation performance for large separation distances between doors.

A recent investigation (Ref. [8]) on evacuation processes of cellular automata suggests that five distances should be taken into account when studying the evacuation performance: the total width of the openings (that is, adding the widths of each door), the doors separation distance, the width difference between the two doors, and the distance to the nearest corner.

From the results shown in Ref. [8], the evacuation time depends on the total width of the openings (if both doors have the same width). But, for a fixed total width of the opening, it appears that the optimal location of the exits depends on the doors separation distance.

Our investigation focuses on symmetric configurations with equally sized doors. At variance to the above mentioned literature, we examine the evacuation dynamics by means of the Social Force Model (SFM). An overview of this model can be found in Section 2.

In Section 3 we describe the specific settings for the evacuation processes. The measurement conditions for the simulations can also be found there.

In Sections 4.1 to 4.2.2 the single door configuration is revisited. Its purpose is to make easier the understanding of the two-doors configuration for very small separation distances d_g.

In Section 4.3 we examine the case of two separated doors. We explore the effect of increasing the separation distance d_g until the clogging areas close to each door become almost independent.

Section 5 resumes the pedestrians behavioural patterns, and its consequences on the evacuation performance, for the different door separation scenarios.

2. Background

2.1. The Social Force Model

The "social force model" (SFM) deals with the pedestrians behavioural pattern in a crowded environment. The basic model states that the pedestrians motion is controlled by three kind of forces: the "desire force", the "social force" and the "granular force". The three are very different in nature, but enter into an equation of motion as follows

$$m_i \frac{d\mathbf{v}^{(i)}}{dt}(t) = \mathbf{f}_d^{(i)}(t) + \sum_j \mathbf{f}_s^{(ij)}(t) + \sum_j \mathbf{f}_g^{(ij)}(t) \tag{1}$$

where m_i is the mass of the pedestrian i, and $\mathbf{v}_i$ is its corresponding velocity. The subscript j represents all other pedestrians (excluding i) and the walls. $\mathbf{f}_d$, $\mathbf{f}_s$ and $\mathbf{f}_g$ are the desire force, the social force and the granular force, respectively. See Refs. [10, 9, 11, 12, 13] for details.

The desire force reflects the pedestrian's own desire to go to a specific place [10]. He (she) needs to accelerate (decelerate) from his (her) current velocity, in order to achieve his (her) own willings. As he (she) reaches the velocity that makes him (her) feel comfortable, no further acceleration (deceleration) is required. This velocity is the "desired velocity" of the pedestrian $\mathbf{v}_d(t)$. The expression for $\mathbf{f}_d$ in Eq. (2) handles this issue.

$$\begin{cases} \mathbf{f}_d^{(i)}(t) &= m_i \dfrac{\mathbf{v}_d^{(i)}(t) - \mathbf{v}_i(t)}{\tau} \\ \mathbf{f}_s^{(ij)} &= A_i\, e^{(r_{ij}-d_{ij})/B_i} \mathbf{n}_{ij} \\ \mathbf{f}_g^{(ij)} &= \kappa\, g(r_{ij}-d_{ij})\, \Delta\mathbf{v}_{ij} \cdot \mathbf{t}_{ij} \end{cases} \tag{2}$$

τ means a relaxation time. Further details on each parameter can be found in Refs. [10, 9, 11, 12, 13].

Notice that the desired velocity $\mathbf{v}_d$ has magnitude v_d and points to the desired place at the direction $\hat{\mathbf{e}}_d$. Thus, v_d represents his (her) state of anxiety, white $\hat{\mathbf{e}}_d$ indicates the place where he (she) is willing to go. We assume, for simplicity, that v_d remains constant during an evacuation process, but $\hat{\mathbf{e}}_d$ changes according to the current position of the pedestrian.

The social force $\mathbf{f}_s$ corresponds to the tendency of each individual to keep some space between him and other pedestrians, or, between him and the walls [14]. The $\mathbf{f}_s$ expressed in Eq. (2) depends on the inter-pedestrian distance d_{ij}. The magnitude $r_{ij} = r_i + r_j$ is the sum of the pedestrian's radius, while A_i and B_i are two fixed parameters ($r_j = 0$ for the interaction with the wall). Thus, $\mathbf{f}_s$ is a repulsive monotonic force that resembles the pedestrian feelings for preserving his (her) *private sphere* [10, 14].

The granular force $\mathbf{f}_g$ appearing in Eq. (1) represents the sliding friction between contacting people (or between people and walls). Its expression can be seen also in Eq. (2). It is assumed to be a linear function of the relative (tangential) velocities $\Delta\mathbf{v}_{ij} \cdot \mathbf{t}_{ij}$ of the contacting individuals. The function $g(r_{ij} - d_{ij})$ returns the argument value if $r_{ij} > d_{ij}$, while κ is a fixed parameter (see Refs. [10, 9, 11, 12, 13]).

2.2. Clustering structures

The time delays during an evacuation process are related to clustering people as explained in Refs. [9, 11]. Groups of pedestrians can be defined as the set of individuals that for any member of the group (say, i) there exists at least another member belonging to the same group (j) in contact with the former. That is,

$$i \in \mathcal{G} \Leftrightarrow \exists j \in \mathcal{G}/d_{ij} < r_i + r_j \tag{3}$$

where $\mathcal{G}$ corresponds to any set of individuals. This kind of structure is called a *human cluster*.

From all human clusters appearing during the evacuation process, those that are simultaneously in contact with the walls on both sides of the exit

are the ones that possibly *block* the way out. Thus, we are interested in the minimum number of contacting pedestrians belonging to this *blocking cluster* that are able to link both sides of the exit. We call this minimalistic group as a *blocking structure*. Any blocking structure is supposed to work as a barrier for the pedestrians in behind.

2.3. The local pressure on the pedestrians

The pressure on a single pedestrian (say, i) is defined as [10]

$$P_i = \frac{1}{2\pi r_i} \sum_{j=1}^{N-1} \mathbf{f}_s^{(ij)} \cdot \mathbf{n}_{ij} \tag{4}$$

$\mathbf{f}_s^{(ij)}$ are the forces acting on the individual i due to the other individuals. Recall that these forces point from any individual j to the individual i, and thus, the products $\mathbf{f}_s^{(ij)} \cdot \mathbf{n}_{ij}$ are always positive.

Notice that Eq. (4) holds either if the pedestrians are in contact or not. The feelings for preserving the *private sphere* actuate as a "social pressure" that makes possible for the individuals to change their behavioural pattern when they come too close to each other or to the walls.

A more formal definition for the "social pressure" is given in Appendix A. We show that the definition (4) is in accordance with the one in Appendix A, if the momentum p_i of the individuals become neglectable. Thus, the expression (4) is suitable for clogging situations where the pedestrians move slowly.

We further applied the formal definition for the "social pressure" to a simple example in Appendix B. We also checked that both definitions give the same results all through Section 4.

3. Numerical simulations

3.1. Geometry and process simulation

We simulated different evacuation processes for room sizes of 20 m $\times$ 20 m, 30 m $\times$ 30 m and 40 m $\times$ 40 m. The rooms had one or two exit doors

on the same wall, as shown in Fig. 1. The doors were placed symmetrically from the mid position of the wall, in order to avoid corner effects. Both doors had also the same width.

At the beginning of the process, the pedestrians were all equally separated in a square arrangement. The occupancy density was initially set to 0.6 people/m^2, close to the allowed limiting values by current regulations [15]. They all had random velocities resembling a Gaussian distribution with null mean value. The pedestrians were willing to go to the nearest exit. Thus, all the pedestrians had the desired velocity $\mathbf{v}_d$ pointing to the same exit door if only one door was available, or to the nearest door if two exits were available.

In order to focus on the effects due to dual exits, we only allowed the pedestrians to move individualistically, that is, neither leaderships nor herding behaviors were present during the evacuation process. At any time, the pedestrians knew the doors location and tried to escape by their own.

The simulations were supported by LAMMPS molecular dynamics simulator with parallel computing capabilities [16]. The time integration algorithm followed the velocity Verlet scheme with a time step of 10^{-4} s. All the necessary parameters were set to the same values as in previous works (see Refs. [12, 13]). It was assumed that all the individuals had the same radius ($r_i = 0.3$ m) and weight ($m_i = 70$ kg). We ran 30 processes for each panic situation, in order to get enough data for mean values computation.

Although the LAMMPS simulator has the most common built-in functions, neither the social force $\mathbf{f}_s$ nor the desire force $\mathbf{f}_d$ were available. We implemented special modules (with parallel computing compatibilities) for the $\mathbf{f}_s$ and $\mathbf{f}_d$ computations. These computations were checked over with previous computations.

The pedestrian's desired direction $\hat{\mathbf{e}}_d$ was updated at each time step. After leaving the room, they continued moving away. No re-entering mechanism was allowed.

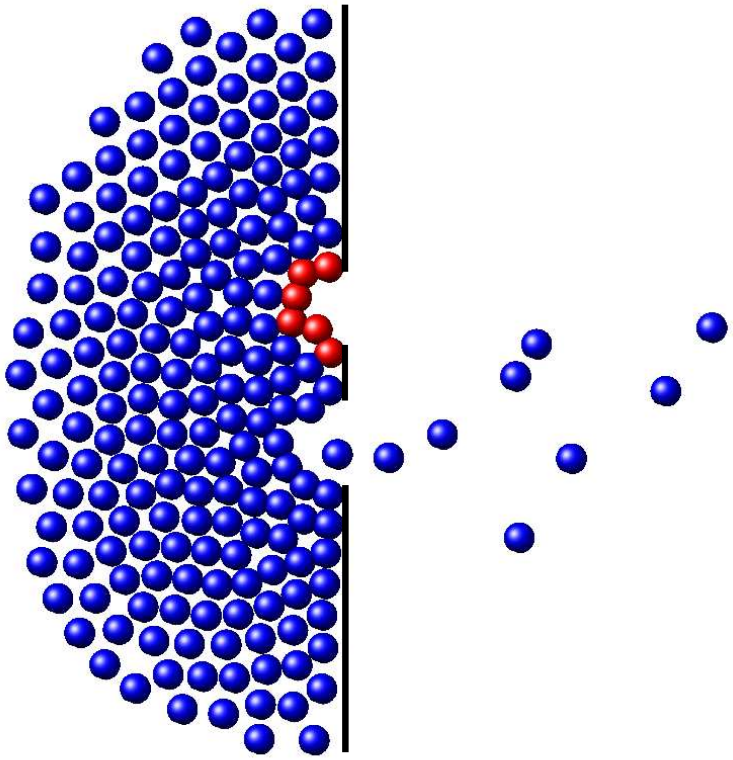

Figure 1: Snapshot of an evacuation process from a $20\,\mathrm{m} \times 20\,\mathrm{m}$ room, with two doors. In red we can see a blocking structure around the upper door. The desired velocity was $v_d = 4\,\mathrm{m/s}$.

3.2. Measurements conditions

Simulations were run in the same way as in Refs. [12, 13]. Each process started with all the individuals inside the room. The measurement period lasted until 80% of the occupants left the room. If this condition could not be fulfilled within the first 3000 s, the process was stopped. Data was recorded at time intervals of 0.05 s (cf. Eq. (2a)).

The simulations ran from relaxed situations ($v_d < 2\,\mathrm{m/s}$) to very stressing rushes ($v_d = 8\,\mathrm{m/s}$). We registered the individuals positions and velocities for each evacuation process. Thus, we were able to compute the "social pressure" through out the process and to trace the pedestrians behavioural pattern.

4. Results

4.1. The faster is slower effect

As a starting point, we checked over the "faster is slower" effect for the room with two doors on the same wall. Fig. 2 shows the recorded evacuation time when the doors are separated a distance of $d_g = 1\,\mathrm{m}$ and when no separation exists at all ($d_g = 0$). The latter means a single opening with width equal to two doors. Both cases (with or without separation) exhibit a change in their corresponding slopes. Thus, the "faster is slower" effect is achieved following the same qualitative response as the one found in previous works for rooms with a single exit [10, 9].

The evacuation time for separated doors in Fig. 2 is always above the time required to evacuate the pedestrians through the single opening (*i.e.* null separation). For $v_d = 6\,\mathrm{m/s}$, the single opening improves the evacuation performance in half of the time that demands the $d_g = 1\,\mathrm{m}$ separation configuration. Other separation distances (not shown) exhibit the same qualitative pattern as the example presented in Fig. 2. Therefore, it is clear that while the total width of the opening remains unchanged, splitting this width into to symmetric exits affects significantly the evacuation performance.

We made further research on the $d_g = 0$ and $d_g > 0$ scenarios. The former is investigated in Section 4.2, while the latter is left to Section 4.3.

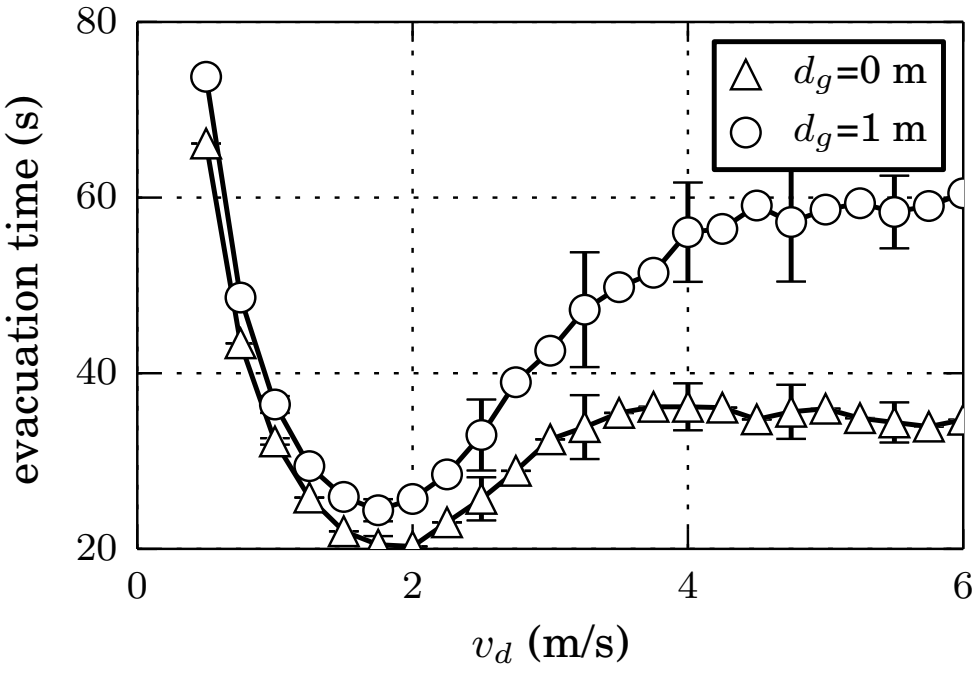

Figure 2: Mean evacuation time for 160 individuals (seconds) vs. the pedestrian's desired velocity (m/s). The room was 20×20 m size. Two contiguous doors were placed on one side of the room as shown in Fig. 1 (see text for details). Mean values were computed from 30 evacuation processes. Each door was $d_w = 1.2$ m width. The desired velocity was $v_d = 4$ m/s. Two situations are shown: $\triangle$ corresponds to the null separation distance between doors, meaning a single door of $2d_w$ width. $\bigcirc$ corresponds to the 1 m separation distance between doors ($d_g = 1$ m).

4.2. The single door vs. the null separation

Recall that the $d_g = 0$ scenario corresponds to a single opening, but the total width of the opening is twice the width of a single door (see Section 4.1). Actually, it resembles the situation of a double sheet door.

4.2.1. The stop-and-go process

Fig. 3 illustrates on how the evacuation performance improves as the opening becomes wider. Fig. 3a corresponds to the single door ($d_w = 1.2\,\mathrm{m}$), while Fig. 3b corresponds to a wider opening ($3d_w = 3.6\,\mathrm{m}$), resembling a multi-leaf opening. Both figures represent the time evolution of a single pedestrian during an evacuation process. We can see the (normalized) pressure acting on the pedestrian and his (her) corresponding velocity. The starting point of the pedestrian was $(x, y) = (12.35\,\mathrm{m}, 8.45\,\mathrm{m})$. Notice that an increase in the opening width from d_w to $3d_w$ (Fig. 3a and Fig. 3b, respectively) reduces the evacuation time by one-fifth approximately.

The pedestrian represented in Fig. 3 increases his (her) velocity towards an asymptotic value at the beginning of the processes. This value corresponds to the desired velocity $v_d = 4\,\mathrm{m/s}$. But close to $t = 2\,\mathrm{s}$, the pedestrian suddenly stops because of the clogging around the exit. Clogging is also responsible for the pressure increase, as shown in both Fig. 3a and Fig. 3b. This can be checked over by means of Eq. (2) because when the velocity of the pedestrian vanishes, the desire force $\mathbf{f}_d$ attains a maximum (in panic situations only). Notice, however, that any further fluctuation of the pressure acting on the pedestrian corresponds to an inverse fluctuation on the velocity. Thus, the pedestrian is able to reach the exit following a stop-and-go process.

The instantaneous pressure acting on a single pedestrian can be computed from Eq. (4) for a slow moving pedestrian (that is, $p_i \simeq 0$). The maximum pressure values $\mathrm{P_{max}}$ in Fig. 3a and Fig. 3b are 8550 $\mathrm{N.m^{-1}}$ and 6475 $\mathrm{N.m^{-1}}$, respectively. The corresponding mean pressure values (after the first 2 s) are 80% and 55% of the respective maximum values. This means that the mean pressure value for the $3d_w$ situation is lower than the corresponding mean value for the d_w situation. That is, the wider opening seems to release pressure from time to time. Consequently, the stop-and-go processes are somehow different for the single door with respect to the $d_g = 0$ situation

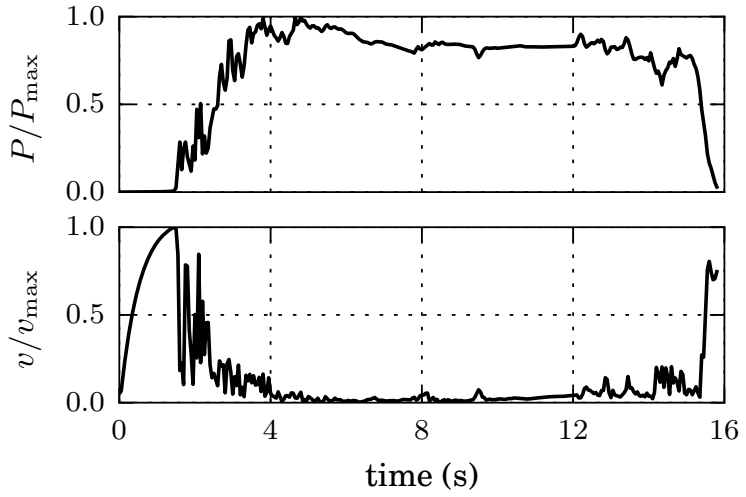

(a) Opening of $d_w = 1.2$ m width.

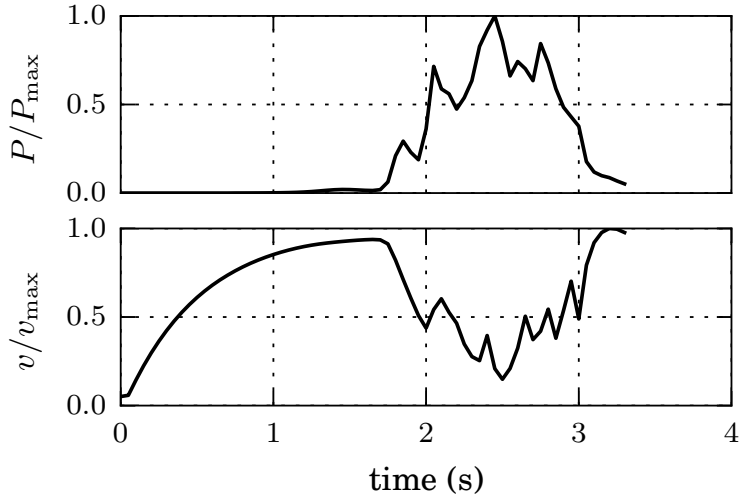

(b) Opening of $3d_w = 3.6$ m width.

Figure 3: Normalized pressure and velocity on a single pedestrian during an evacuation process. Data was recorded from the the initial position at $x = 12.35$ m and $y = 8.45$ m, until the individual left the room ($x > 20$ m). The pedestrians desired velocity was $v_d = 4\,\mathrm{m/s}$. Two situations are shown: (a) evacuation through a single door of width $d_w = 1.2$ m. (b) evacuation through an opening of $3d_w = 3.6$ m.

(the wider opening).

The above analyses corresponds to a single pedestrian moving along the middle of the room. It does not hold for the whole crowd. For details on the pressure patterns of the crowd, see Section 4.2.2.

4.2.2. The pressure and stream patterns

For a better understanding on how the pedestrians are (intermittently) released from high pressures in the wide opening situation, we pictured the whole scene into a pressure contour map and a mean stream path map for all the individuals. Fig. 5c shows the pressure levels (P_i) for the clogging area. The warm colors are associated to high pressure values. These values are close to the corresponding maximum pressure values (not shown). Thus, the warm regions define the places where the pedestrians slow down most of the time. They are expected to get released only for short periods of time. On the contrary, the regions represented in cold colors (low mean pressure) are those where the individuals are able to get released for longer time periods.

Fig. 4c represents the mean stream lines during the evacuation process. It completes the stop-and-go picture since it exhibits the released paths for leaving the room. Notice that the stream lines pass through the low pressure regions. That is, it can be seen in Fig. 4c that the stream lines gather along the middle of the clogging area, where "cold" pressure colors can be found (cf. Fig. 5c). The "warm" pressure colors are placed on the sides of this region.

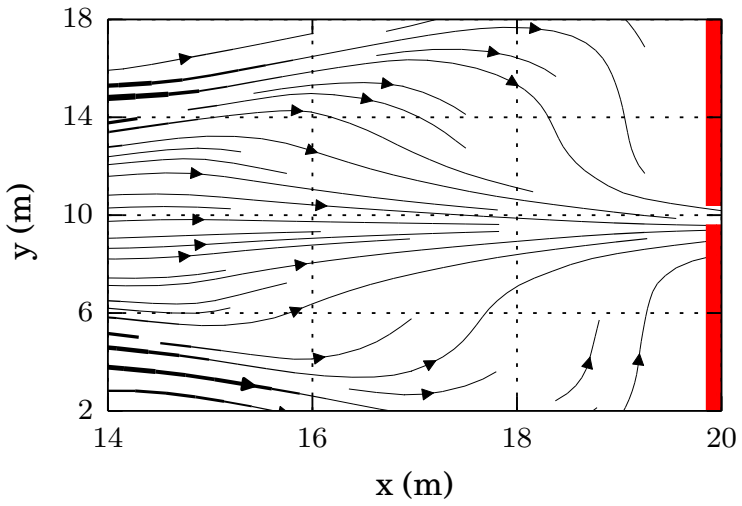

307

(a) Opening of $d_w = 1.2$ m width.

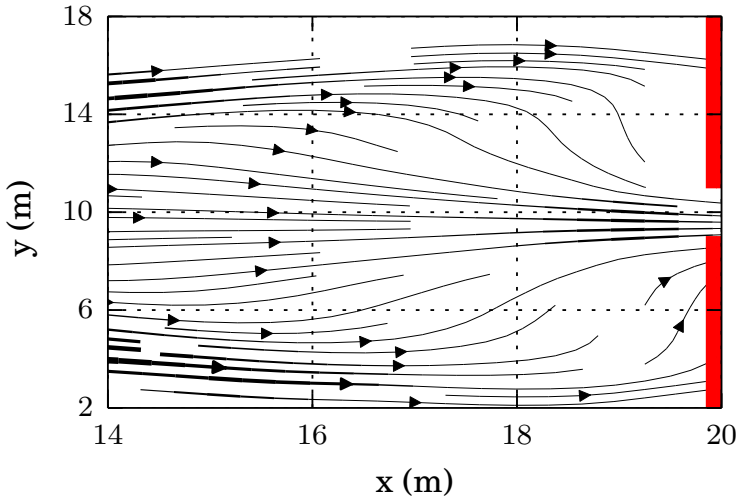

308

(b) Opening of $2d_w = 2.4$ m width.

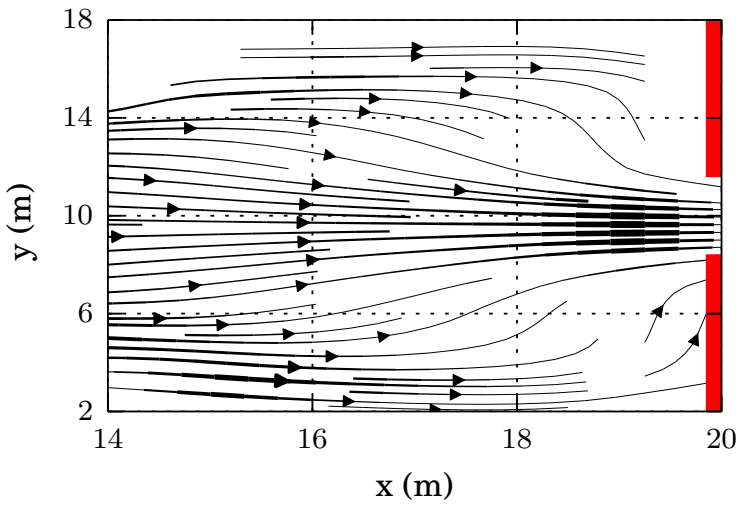

(c) Opening of $3d_w = 3.6$ m width.

Figure 4: Mean stream lines computed from 30 evacuation processes until 100 pedestrians left the room ($20\,\mathrm{m} \times 20\,\mathrm{m}$ size). The lines connect the normalized velocity field ($v/v_{\max}$). The arrows indicate the stream direction. Data was recorded on a square grid of $1\,\mathrm{m} \times 1\,\mathrm{m}$ and then splined to get smooth curves. The red lines at $x = 20$ m represent the walls on the right of the room. The pedestrian's desired velocity was $v_d = 4\,\mathrm{m/s}$ for all the cases.

We checked over the trajectory of the single pedestrian represented in Fig. 3b and we observed that he (she) managed to get out of the room through the path where the stream lines get denser. Thus, Fig. 3b resembles the stop-and-go process for the pedestrians passing through the middle of the clogging area, that is, along the low pressure (middle) region. The pedestrians on the sides of this region (high pressure region) are expected to slow down since Fig. 4c shows no stream lines to the exit.

Recalling the results in Fig. 3a for the same single individual as in Fig. 3b, we realize that the single door scene is likely to differ from the $d_g = 0$ situation since both patterns (for the same individual) do. Thus, we examined the pressure contour map for the single door and for an opening of twice the single door width. The results are shown in Fig. 5. Fig. 5b exhibits a similar pressure map pattern as Fig. 5c, but the single door pressure map in Fig. 5a does not. For the single door situation, we do not observe the lower pressure pathway in the middle of the clogging area. Instead, high pressure

is acting on the pedestrians, as shown in the (normalized) pressure evolution in Fig. 3a. The corresponding velocity evolution (Fig. 3a) informs that the pedestrians in this region experience a slow down.

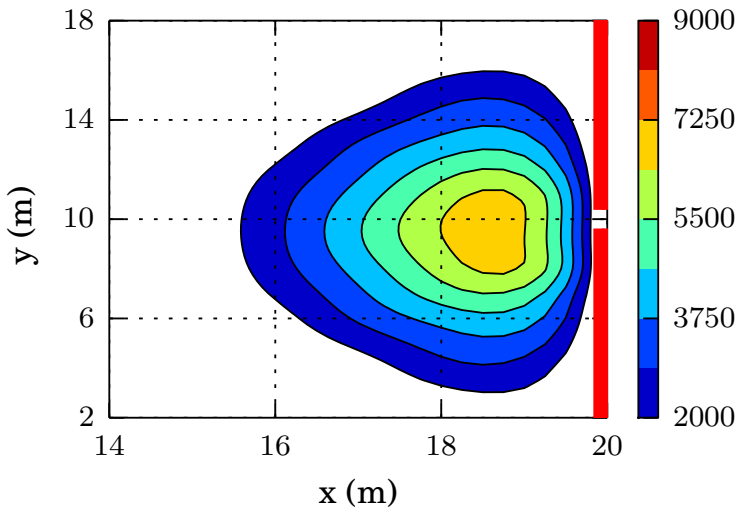

(a) Opening of $d_w = 1.2$ m width.

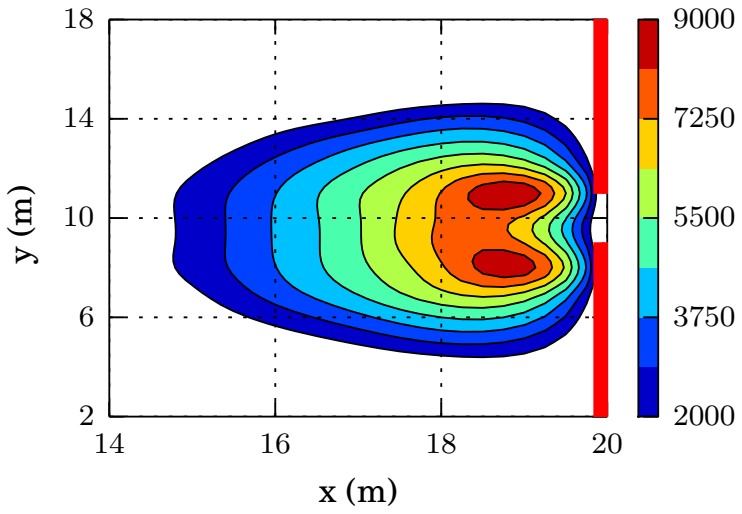

(b) Opening of $2d_w = 2.4$ m width.

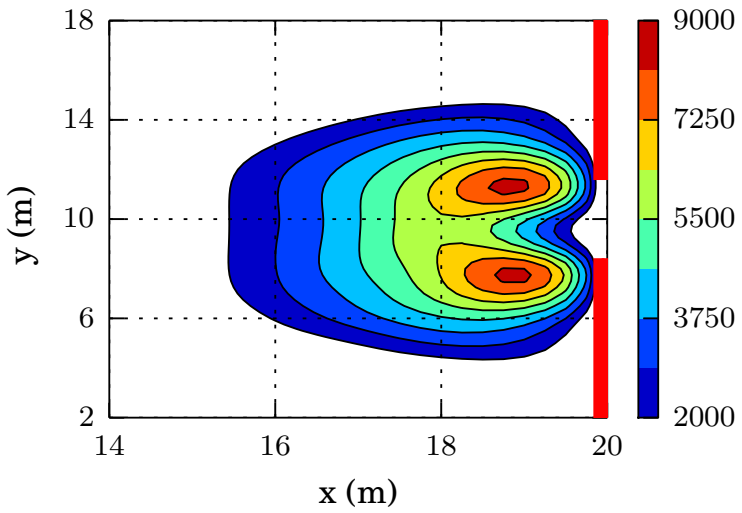

(c) Opening of $3d_w = 3.6$ m width.

Figure 5: Mean pressure contour lines computed from 30 evacuation processes until 100 pedestrians left the room (20 m × 20 m size). The scale bar on the right is expressed in N.m^{-1} units (see text for details). The red lines at $x = 20$ m represent the walls on the right of the room. The pedestrian's desired velocity was $v_d = 4$ m/s. The contour lines were computed on a square grid of 1 m × 1 m and then splined to get smooth curves. Level colors can be seen in the on-line version only.

Notice, once again, that the results shown in Figs. 3 only resembles the situation in the middle of the room. Figs 4c and Figs. 5 exhibit the situation for the whole crowd. However, the mid path in "cold" colors in 5c is the most meaningful region to our research, since it completes the picture for the stop-and-go process, firstly evidenced in Fig. 3b.

At this stage of the investigation we are able to point out a few conclusions. The widening of the single door increases the pedestrian's flux, as asserted in Ref. [7]. In the narrow situation (see Fig. 3a), the pedestrians experience a slow down. The corresponding time delays have been associated to blocking structures (see Refs. [9, 11]) and causes the pressure acting on the nearby individuals to rise. Fig. 5a resembles this situation. However, as the opening widens (*i.e.* the null separation situation), the pressure pattern changes qualitatively (see Fig. 5c and Fig. 5b), allowing the pedestrians in the middle of the clogging area to make a pathway to the exit. This pathway corresponds to the breaking of the blocking structures.

4.3. Separated doors

We will now analyze the case in which the evacuation process is through two doors, symmetrically placed on the same side of the room. We will explore the dependence of such a process on the doors separations. We will assume that each door width is $d_w = 1.2\,\mathrm{m}$.

It has been shown in Fig. 2 that separating the doors a distance $d_g = 1\,\mathrm{m}$ worsens the evacuation performance with respect to the null separation. We further explored this worsening by increasing d_g at steps of $0.5\,\mathrm{m}$, starting from the null separation distance. Fig. 6 shows the mean evacuation time and the corresponding error bars (indicating the $\pm\sigma$ limits). The desired velocity was set to $v_d = 4\,\mathrm{m/s}$, where the "faster is slower" effect takes place.

The evacuation time as a function of d_g shown in Fig. 6 is one of our main results. The worsening in the evacuation performance rises to a maximum value at $1\,\mathrm{m}$ while its slope changes sign for $d_g > 1\,\mathrm{m}$. Thus, $d_g = 1\,\mathrm{m}$ appears to be the worst evacuation scenario for the $20\,\mathrm{m} \times 20\,\mathrm{m}$ room with 225 individuals and two doors of $d_w = 1.2\,\mathrm{m}$ each (see Fig. 6).

We further computed the mean evacuation time for an increasing number of pedestrians (and room sizes). We kept the pedestrian density unchanged (at $t = 0$) for all the simulation processes. Fig. 7 exhibits the mean evacuation time per pedestrian as a function of the separation distance (*i.e.* gap). We divided the evacuation time by the total number of pedestrians for visualization reasons.

The results shown in Fig. 7 were not expected. The evacuation time settles to an asymptotic value for separation distances $d_g > 5\,\mathrm{m}$. The mean evacuation time becomes almost independent of the separation distances d_g despite that the clogging areas around the doors might still overlap.

Fig. 7 also shows that the slope not always changes sign at $d_g \simeq 1\,\mathrm{m}$. Furthermore, as the number of pedestrians is increased for $d_g > 1\,\mathrm{m}$, the evacuation time slope raises to positive values. The greater the number of pedestrians, the worst the evacuation time (per individual). This appears to occur for $d_g > 1\,\mathrm{m}$, regardless of the crowd size. That is, according to

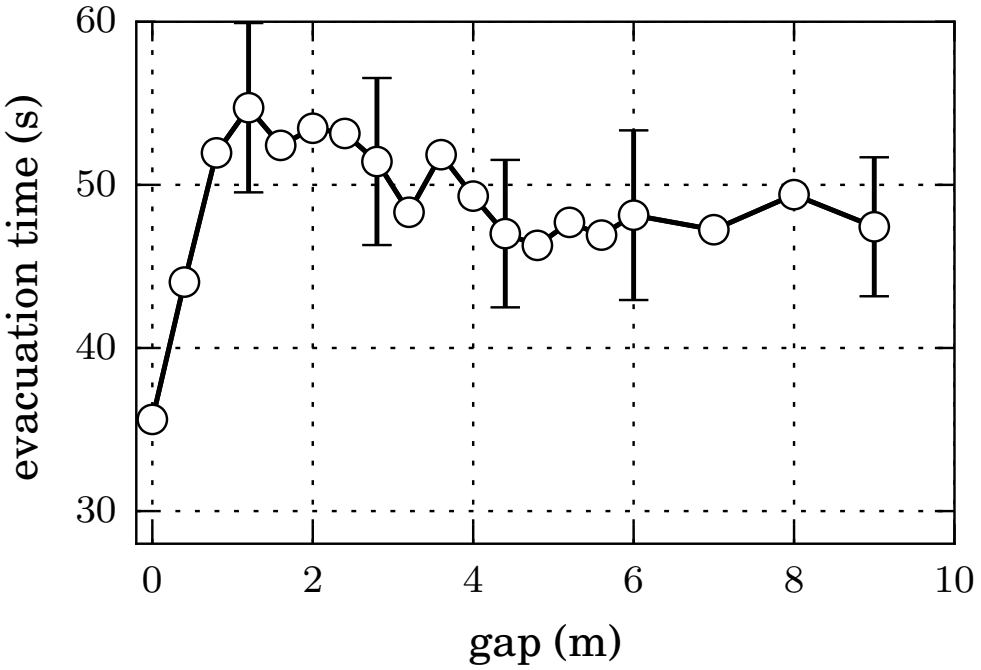

Figure 6: Mean evacuation time for 225 pedestrians (room of 20×20 m size) as a function of the doors separation distance. Mean values were computed from 30 evacuation processes until 160 pedestrians left the room. Each door was $d_w = 1.2$ m width for non-vanishing gaps. The null gap means a single door of $2d_w$ width. The desired velocity was $v_d = 4\,\mathrm{m/s}$.

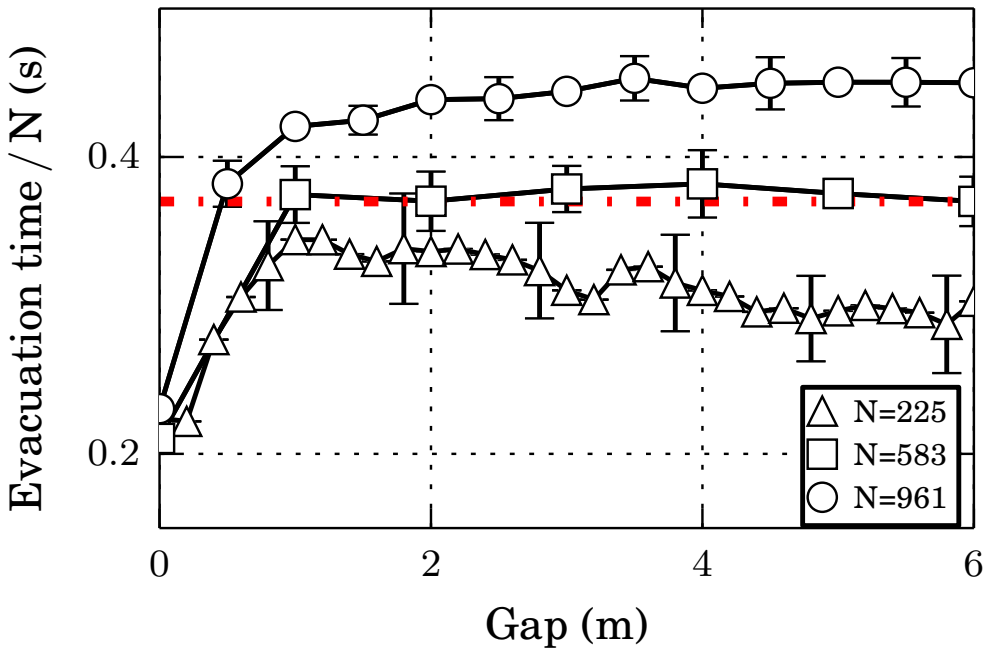

Figure 7: Mean evacuation time per total number of pedestrians that left the room (N), as a function of the doors separation distance. Mean values were computed from 30 evacuation processes. Each door was $d_w = 1.2$ m width for non-vanishing gaps. The null gap means a single door of $2d_w$ width. Three situations are shown: △ corresponds to the 20×20 m room when 160 pedestrians left the room, □ corresponds to 30×30 m room when 530 pedestrians left the room, and ◯ corresponds to 40×40 m room when 865 pedestrians left the room. The desired velocity was $v_d = 4\,\mathrm{m/s}$.

Fig. 7, there exists a separation distance value $d_g \simeq 1\,\mathrm{m}$ where the evacuation slope changes sharply to negative or positive values (for $d_g > 1\,\mathrm{m}$). This phenomenon has not been studied in the literature, to our knowledge.

We can resume the results in Fig. 7 in the following way: the evacuation time rises when the doors separation increases from a wide opening (null separation distance) to the distance $d_g \simeq 1\,\mathrm{m}$. At this gap, the evacuation time slope changes notably, entering a much slowly varying regime towards an asymptotic value (for $d_g \gg 1\,\mathrm{m}$). The former can be identified as a regime for small values of d_g, while the latter is valid for moderate to large values of d_g. The fact that a sharp change occurs at $d_g \simeq 1\,\mathrm{m}$, no matter the crowd size, suggests that both regimes are somehow different in nature. This moved us to explore the two regimes separately.

4.3.1. The regime for $d_g < 1\,m$

Our starting point is the pressure contour map, since we can easily compare the current patterns with those presented in Section 4.2.2. Fig. 8a shows the mean pressure pattern for the separation distance $d_g = 1.5\,\mathrm{m}$, that is, close to the gap value where the sharp change in the slope occurs. The differences between Fig. 8a and Fig. 5 are noticeable. We can now see a wide region in the center of the clogging area representing the high pressure (P_i) acting on each pedestrian (warm colors in Fig. 8a). The regularity in the colors of this region is meaningful: the high pressure acting on the pedestrians does not allow a regular stream (pathway) to the exit. This is in agreement with the evacuation time worsening shown in Fig. 6.

In all cases the pressure maps showed a resemblance with the ones reported in [17]

Fig. 8a suggests that blocking structures might be present for long time periods, since the pedestrians cannot manage to get out easily. We examined this possibility through the *blocking probability*. In this context, the blocking probability is associated to the ratio between the time that each door remains blocked with respect to the total evacuation time (cf. Section 2.2). Fig. 9 presents two kinds of blockings: the simultaneous blocking of both doors, and the blocking of a single door (say, the one on the left). The former connects the left most wall with the right most wall, but does not contact the separation wall in the middle of the walls. The latter connects the walls on

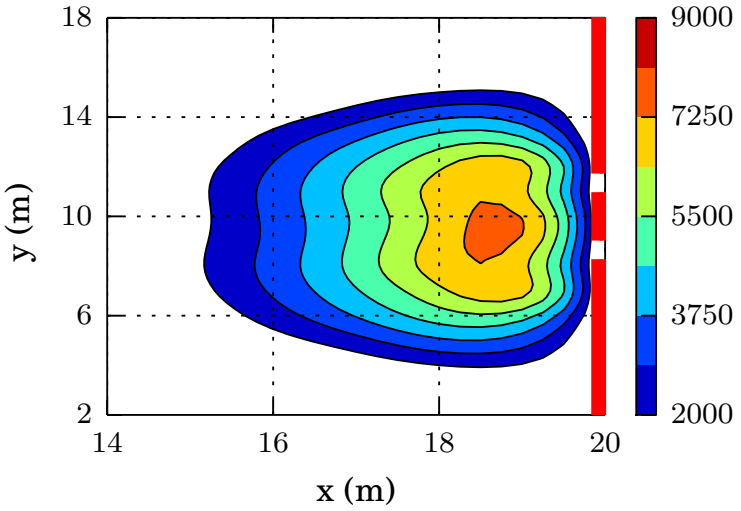

(a) Separation distance of $d_g = 1.5$ m.

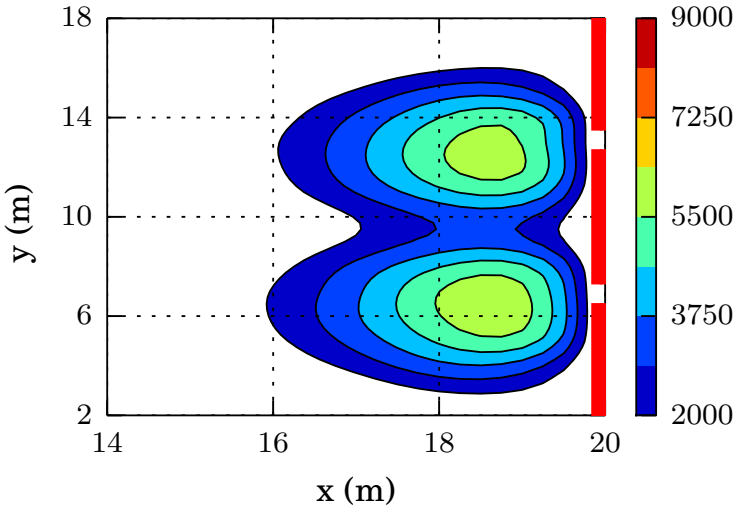

(b) Separation distance of $d_g = 5$ m.

Figure 8: Mean pressure contour lines computed from 30 evacuation processes until 100 pedestrians left the room (20 m × 20 m size). The scale bar on the right is expressed in N.m^{-1} units (see text for details). The red lines at $x = 20$ m represent the walls on the right of the room. The pedestrian's desired velocity was $v_d = 4$ m/s. The contour lines were computed on a square grid of 1 m × 1 m and then splined to get smooth curves. Level colors can be seen in the on-line version only.

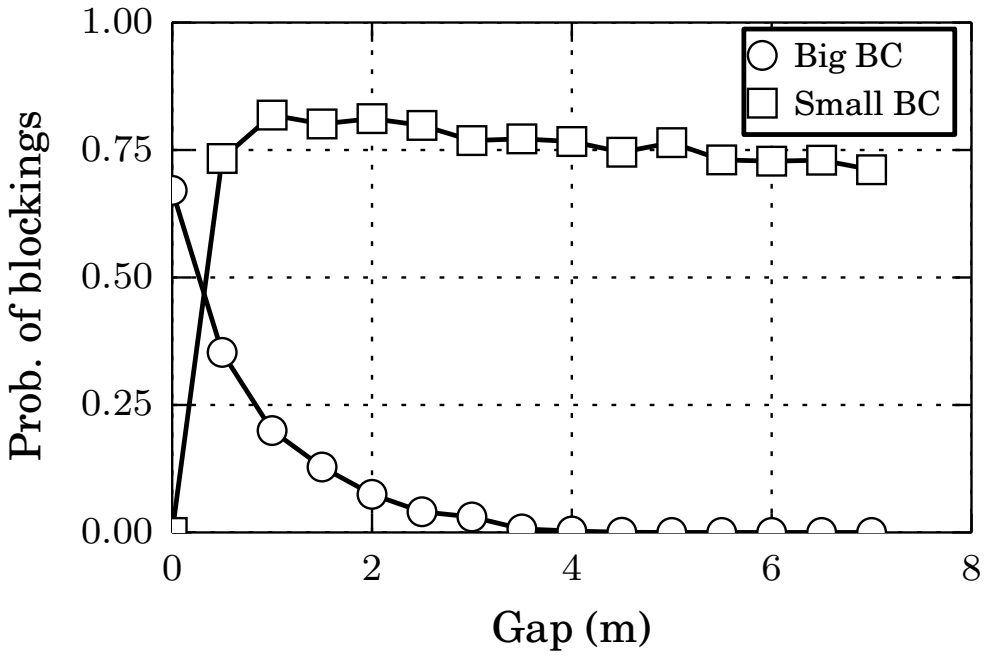

Figure 9: Ratio between time steps including blocking structures and the total number of time steps for 30 evacuation processes, as a function of the doors separation distance. The room size was 20×20 m with 225 occupants. Each door was $d_w = 1.2$ m width for non-vanishing gaps. The null gap means a single door of $2d_w$ width. The desired velocity was $v_d = 4\,\mathrm{m/s}$. ◯ corresponds blocking structures connecting both the left side wall of the left door with the right side wall of the right door (see text for details). □ corresponds to blocking structures connecting both sides of a single door (see text for details).

both sides of the selected door (say, the one on the left).

According to Fig. 9, the single door blockings are not relevant until $d_g \simeq 1\,\mathrm{m}$, while the simultaneous blockings weaken as the gap (separation distance d_g) increases. The single door blockings resemble the response in Fig. 6, and thus, we conclude that this kind of blockings should play an important role in the increase of the evacuation time for small gaps d_g. Notice that single door blocking probability explains the 75% of the evacuation time, as can be seen in Fig. 9.

The results so far moved us to focus closer on the dynamics around each

door. We watched many animations of the evacuation process for gap distances between the null separation to $d_g = 1.5\,\mathrm{m}$ (not shown). We realized that single door blockings hold if the gap is large enough to accommodate at least two pedestrians. That is, any blocking structure enclosing a single door can hold for some time if the pedestrians at the end of the structure (and in contact with the walls) do hardly leave the structure. Two pedestrians are needed at the gap wall to ensure that both doors remain blocked.

We want to call the attention on the fact that when d_g passes through the 1 m situation, the kind of simultaneous blocking without contacting the gap wall, is replaced by the kind of single door blockings acting (usually) simultaneously. This achieves a qualitative different pressure and stream pattern. As shown in Fig. 5b, the widening of the exit allows a pathway through the middle of the clogging area. This is likely to occur even for very small gaps (see Fig. 9). However, the single door blockings follow a pressure pattern similar to Fig. 5a on each door. What we see in Fig. 8a is the combined pattern built from two single door patterns as in Fig. 5a.

We conclude from the analysis of small gaps ($d_g < 1\,\mathrm{m}$) that a door separation distance roughly equal to two pedestrian widths is critical. This distance allows persistent single door blockings. Small distances (close to the null separation) do not actually allow single door blockings to hold for long time. Thus, the role of $d_g = 2r_{ij}$ (two pedestrian's width) is decisive to move the evacuation process from one regime to another.

4.3.2. The regime for $d_g > 1\,m$

Fig. 9 shows that the single door blockings (see Section 4.3.1) remains around 75% of the total evacuation time for $d_g > 1\,\mathrm{m}$ (225 individuals in the room). We also computed this magnitude for situations with increasing number of individuals (see Fig. 10). The probability of single door blockings approaches unity as the crowd size increases. This means, according to our definition of blocking probability, that the blocking time raises as the number of individuals increases. The gap distance, however, does not play a significant role for $d_g > 1\,\mathrm{m}$.

There is a noticeable difference between the evacuation time shown in Fig. 7 and the blocking probability exhibited in Fig. 10. Fig. 7 presents

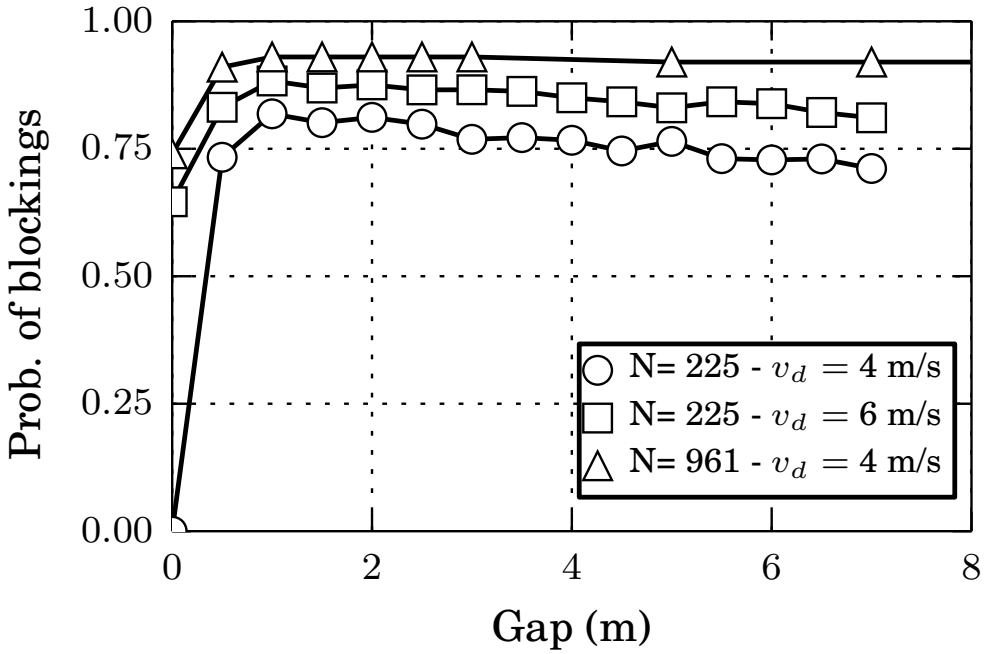

Figure 10: Ratio between time steps including blocking structures and the total number of time steps for 30 evacuation processes, as a function of the doors separation distance. The only blocking structures considered were those connecting both sides of one single door (see text for details). Each door was $d_w = 1.2$ m width for non-vanishing gaps. The null gap means a single door of $2d_w$ width. Three scenarios are shown: ◯ corresponds to the room of size 20×20 m with 225 occupants and a desired velocity of $v_d = 4\,\mathrm{m/s}$. □ corresponds to the room of size 20×20 m with 225 occupants and a desired velocity of $v_d = 6\,\mathrm{m/s}$. △ corresponds to the room of size 40×40 m with 961 occupants and a desired velocity of $v_d = 4\,\mathrm{m/s}$.

the evacuation time for three different room sizes and increasing number of pedestrians. The slope of the evacuation curve is negative for the $20 \times 20\,\mathrm{m}$ room, it vanishes for the $30 \times 30\,\mathrm{m}$ situation and it becomes slightly positive for the $40 \times 40\,\mathrm{m}$ room (for $d_g > 1\,\mathrm{m}$). Thus, as the number of pedestrians increases, the slope of the evacuation time changes sign. However, this does not occur for the blocking probability (see Fig. 10). The slope of the blocking probability remains always negative for an increasing number of pedestrians (and desire velocities). Therefore, the changes in the slope observed in Fig. 7 cannot be explained by changes in the blocking time (*i.e* blocking probability).

We checked the pressure patterns for $d_g > 4d_w$ (see Fig. 8b as an example). We came to the conclusion that since the evacuation slope in Fig. 7 changes with an increasing number of individuals, the whole bulk should be involved in this phenomenon. Therefore, we focused our investigation on the pressure contribution of the whole bulk.

As shown in Eq. (A.3) of Appendix A , we can realize that the pressure of the whole bulk (left-hand side) is related to the total desire force contribution (right-hand side). Thus, the pressure of the bulk can vary in two possible ways: if the desire force of the individuals (*i.e.* anxiety levels) changes, or, if the crowd size changes. An increase on either the number of evacuating pedestrians (N) or their corresponding anxiety level (v_d), will increase the pressure of the whole bulk. This result is in accordance with the experiment performed by Jose M. Pastor et al. in [18]. A simple example is presented in the Appendix.

Fig. 7 exhibits the evacuation time for an increasing number of pedestrians. But, an increase in the pedestrians anxiety level should resemble similar results, if the above reasonings are true. Fig. 11 shows the evacuation time as a function of the separation distance for two different desired velocities. As expected, the sharp change in the slope occurs around $d_g = 2r_{ij}$. Also the slope changes as the desired velocity (v_d) is increased (*i.e.* higher anxiety level). This confirms that the social pressure is responsible the slope behaviour shown in Fig. 7.

We conclude from the analysis of large gaps ($d_g > 1\,\mathrm{m}$) that the evacuation time is controlled by the social pressure in the bulk. The crowd size

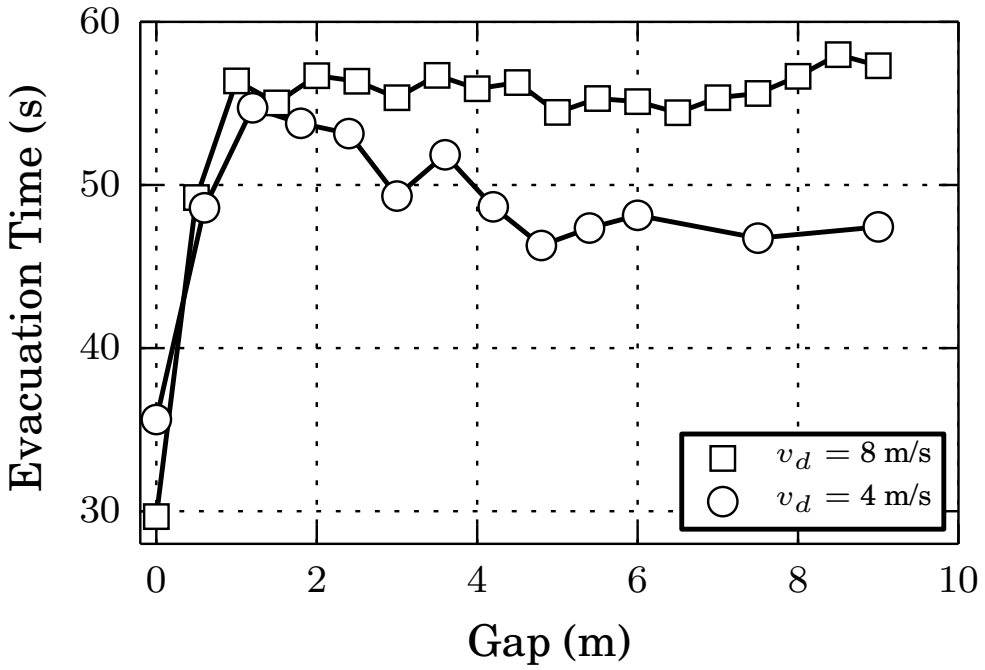

Figure 11: Mean evacuation time for 225 pedestrians (room of 20×20 m size) as a function of the doors separation distance. Mean values were computed from 30 evacuation processes until 160 pedestrians left the room. Each door was $d_w = 1.2$ m width for non-vanishing gaps. The null gap means a single door of $2d_w$ width. ◯ corresponds to pedestrians with desired velocity of $v_d = 4\,\mathrm{m/s}$. □ corresponds to pedestrians with desired velocity of $v_d = 8\,\mathrm{m/s}$.

and the desired velocity v_d affects the pressure acting on the pedestrians. For $d_g > 5\,\mathrm{m}$ in our simulations, the evacuation time is very close to the corresponding asymptotic value, although the bulks around each door are not completely independent. This means that the mixing of both crowds (that is, the fact that the bulks are in contact) do not affect strongly the evacuation performance.

5. Conclusions

We examined in detail the evacuation of pedestrians for the situation where two contiguous doors are available for leaving the room. Throughout Section 4 we presented results on the evacuation performance under high anxiety levels and increasing number of pedestrians. Both conditions exhibit the novel result that a worsening in the evacuation time exists as the door separation distance d_g increases from the null value to roughly the width of two pedestrians. Special situations may enhance the evacuation performance for larger values of d_g.

The range from $d_g = 0$ to $d_g \gg d_w$ was inspected. In the interval $0 \leq d_g \leq 2r_{ij}$ (two pedestrian's width), the evacuation performance worsened for all the explored situations, as the separation distance between doors d_g increased. But, from $d_g > 2r_{ij}$ the evacuation time enhanced for relatively small crowds and moderate anxiety levels. We realized that the sharp change in the evacuation behaviour at $d_g = 2r_{ij}$ corresponded to qualitative differences in the pedestrian dynamics close to the exits.

After a detailed comparison of the dynamics for the single door situation and for two doors very close to each other (that is, $d_g < 2r_{ij}$), we concluded that the blocking structures (*i.e.* blocking arcs) around the openings were released intermittently, allowing the pedestrians to leave the room in a stop-and-go process. As the separation distance approached $2r_{ij}$, the blocking arcs around each door, resembled the blocking situation of two single doors. This changes only affected the local dynamics (close to the doors), while the crowd remained gathered into a single clogging area.

For $d_g > 2r_{ij}$ the single door blocking structures become relevant even for large values of d_g (see Fig. 9). No further qualitative changes were ob-

served locally around each door. However, increasing the crowd size (N) or the pedestrian's anxiety level (v_d) slowed down the evacuation. Both magnitudes are linked to the pressure acting on the pedestrians, and therefore, enhanced the "faster is slower" effects.

For a better understanding of the relationship between N, v_d and the pressure in the bulk, a simple lane example complemented our analysis. It was shown that the classical virial expression is still suitable for the investigation of social systems.

6. Acknowledgments

C.O. Dorso is a main researcher of the National Scientific and Technical Research Council (spanish: Consejo Nacional de Investigaciones Científicas y Técnicas - CONICET), Argentina. G.A. Frank is an assistant researcher of the CONICET, Argentina. I.M. Sticco and S. Cerrotta have degree in Physics.

Appendix A. Alternative definition for the social pressure

Recall that the social force model (SFM) deals with the pedestrians desire and their private space preservation. Although the desire force $\mathbf{f}_d$ is a "unilateral" force, the Newton equations of motion remain valid. Therefore, it can be derived from the virial relation that [19]

$$\Big\langle \sum_{i=1}^{N} \frac{p_i^2}{m_i} + \sum_{i=1}^{N} \mathbf{r}_i \cdot \mathbf{f}_i \Big\rangle = -2\mathcal{P}\mathcal{A} \tag{A.1}$$

for the set of N pedestrians inside an area $\mathcal{A}$. p_i and $\mathbf{f}_i$ are the momentum and total force acting on the individual i (excluding the interaction with the walls). $\langle\cdot\rangle$ corresponds to the mean value along time. The right hand side $-2\mathcal{P}\mathcal{A}$ defines the global pressure on the curve enclosing the surface $\mathcal{A}$.

Following Ref. [19] we can define the "social pressure function" P_i as

$$2P_i\mathcal{A}_i = \frac{p_i^2}{m_i} + \frac{1}{2}\sum_{j=1}^{N-1} \mathbf{r}_{ij} \cdot \mathbf{f}_s^{(ij)} \tag{A.2}$$

where $\mathcal{A}_i$ is the area enclosing the pedestrian i and $\mathbf{r}_{ij} = \mathbf{r}_i - \mathbf{r}_j$. Notice that the inner product $\mathbf{r}_{ij} \cdot \mathbf{f}_s^{(ij)}$ is always positive for repulsive feelings.

The "social pressure function" P_i is roughly similar to the literature definition [10], as expressed in Eq. (4), for neglectable momentum p_i. Furthermore, Eqs. (4) and (A.2) become equal if the area $\mathcal{A}_i$ and r_{ij} are replaced by πr_i^2 and the contacting distance $2r_i$, respectively.

We can further compute the pressure on all the pedestrians according to Eq. (A.1). Notice that the force sum can be split into the summation of three contributions: the desire forces, the social forces and the granular forces. Actually, the granular force does not play a role because of orthogonality ($\mathbf{r}_{ij} \cdot \mathbf{f}_g^{(ij)} = 0$). Consequently, replacing Eq. (A.2) into the virial relation (A.1) gives

$$\sum_{i=1}^{N} \langle 2P_i \mathcal{A}_i \rangle = -2\mathcal{P}\mathcal{A} - \sum_{i=1}^{N} \langle \mathbf{r}_i \cdot \mathbf{f}_d^{(i)} \rangle \tag{A.3}$$

We should remark that Eq. (A.3) holds either if the pedestrians are in contact or not. The "social pressure function" P_i makes possible for the individuals to change their behavioural pattern when they come too close to each other.

Appendix B. The lane example

We decided to open this supplementary section in order to make clear the meaning of the "social pressure" acting on an individual and the collective pressure (that is, the *bulk* pressure) on a set of individuals. We will follow a simple example as a guide for more general situations.

Appendix B.1. The social pressure

Fig. B.12 represents a lane of individuals pushing to the right. The ending wall prevents the individuals from moving. All the pedestrians in the lane are at their equilibrium positions $x_1, x_2, ..., x_i, ...x_N$, while the wall is placed

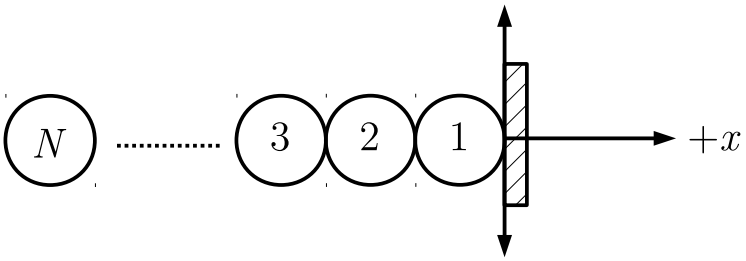

Figure B.12: Lane of individuals pushing to the right. The horizontal axis indicates the positive direction.

at the position $x_0 = 0$ (see Fig. B.12).

The pedestrians push to the right acknowledging a desired force $f_d^{(i)} = mv_d/\tau$, according to Eq. (2). The social repulsion feelings balance this desire force, but only the contacting neighbors are relevant to these feelings. Thus, the balance equation for any pedestrian in the lane reads

$$f_s^{(i,i+1)} - f_s^{(i,i-1)} + \frac{mv_d}{\tau} = 0 \tag{B.1}$$

for $f_s^{(i,j)}$ meaning the repulsive feelings of pedestrian i due to the presence of pedestrian j. Notice that the boundary condition at the wall-end is $x_0 = 0$ (Dirichlet condition), while the condition at the free end is $f_s^{(N,N+1)} = 0$ (Neumann condition). The forces on the pedestrians can be obtained recursively from Eq. B.1, starting at the free ended individual ($i = N$). The resulting expression is

$$f_s^{(i,i-1)} = (N - i + 1)\,\frac{mv_d}{\tau} \quad , \quad i = 1, ..., N \tag{B.2}$$

while the corresponding positions $x_1, x_2, ..., x_i, ...x_N$ are obtained by a backward substitution of the social forces expressed in Eq. (2), starting at the wall-end

$$x_i = x_{i-1} - (r_i + r_{i-1}) + B\,\ln\left[(N - i + 1)\,\frac{mv_d}{A\tau}\right] \tag{B.3}$$

The pressure on a single pedestrian P_i corresponds to the forces acting on him (her) (per unit length) due to the neighboring pedestrians. According to Eqs. (4), the pressure for any individual i in the lane is

$$P_i = \frac{1}{2\pi r_i}\left[f_s^{(i,i+1)} + f_s^{(i,i-1)}\right] \tag{B.4}$$

We can also arrive to this expression through the "social pressure function" definition (A.2)

$$P_i = \frac{1}{2}\left[\frac{x_i - x_{i+1}}{2\mathcal{A}_i}\, f_s^{(i,i+1)} + \frac{x_{i-1} - x_i}{2\mathcal{A}_i}\, f_s^{(i,i-1)}\right] \tag{B.5}$$

where the magnitude $x_{ij}/2\mathcal{A}_i$ corresponds to the (inverse) effective length of the pedestrian. For individuals modeled as circles, the inter-pedestrian distance is roughly $x_{ij} = 2r_i$ and the area is $\mathcal{A}_i = \pi r_i^2$. Thus, both definitions agree. However, the last one is preferred since it does not assume that the forces actuate exactly at the distance r_i, as already mentioned in Section 2.3.

Appendix B.2. The bulk pressure

We can now illustrate on how to compute the virial relation (A.3). We can add the social pressures expressed in (B.5) for the N pedestrians in the lane.

$$\begin{cases} 2P_1\mathcal{A}_1 &= \dfrac{x_1}{2} f_s^{(1,2)} - \dfrac{x_2}{2}\, f_s^{(1,2)} \\ 2P_2\mathcal{A}_2 &= \dfrac{x_2}{2}\left[f_s^{(2,3)} - f_s^{(2,1)}\right] - \dfrac{x_3}{2}\, f_s^{(2,3)} + \dfrac{x_1}{2}\, f_s^{(2,1)} \\ 2P_3\mathcal{A}_3 &= \dfrac{x_3}{2}\left[f_s^{(3,4)} - f_s^{(3,2)}\right] - \dfrac{x_4}{2}\, f_s^{(3,4)} + \dfrac{x_2}{2}\, f_s^{(3,2)} \\ \ldots & \\ 2P_N\mathcal{A}_N &= -\dfrac{x_N}{2}\, f_s^{(N,N-1)} + \dfrac{x_{N-1}}{2}\, f_s^{(N,N-1)} \end{cases} \tag{B.6}$$

These are the local pressures on each pedestrian due to the contacting neighbors (and excluding the wall). Adding the terms results in the virial relation, as expressed in (A.3)

$$\begin{aligned}\sum_{i=1}^{N} 2P_i\mathcal{A}_i &= (x_1 - x_2)f_s^{(1,2)} + (x_2 - x_3)f_s^{(2,3)} + ... \\ &+ (x_{N-1} - x_N)f_s^{(N,N-1)} \\ &= x_1 \frac{N\, mv_d}{\tau} - \sum_{i=1}^{N} x_i \frac{mv_d}{\tau}\end{aligned} \tag{B.7}$$

where the first term on the right corresponds to the global pressure $-2\mathcal{PA}$. Notice that x_1 is negative, and thus, $2\mathcal{PA}$ is defined as a positive magnitude. The last term is also positive, adding pressure to the bulk due to the desire forces.

The virial relation (A.3) allows to compute the *bulk* pressure on a group of pedestrians. For example, the pressure on the M pedestrians closest to the wall corresponds to the force acting on this group due to the other $N - M$ pedestrians. According to Eq. (A.3), the pressure on the M individuals is

$$\sum_{i=1}^{M} 2P_i\mathcal{A}_i = -2\mathcal{PA} - \sum_{i=M+1}^{N} 2P_i\mathcal{A}_i - \sum_{i=1}^{N} x_i \frac{mv_d}{\tau} \tag{B.8}$$

The *bulk* pressure on the first M individuals increases as more individuals are included in the crowd. This can be verified by evaluating Eq. (B.7) and Eq. (B.8) for increasing values of N.

The Eqs. (B.2) and (B.3) allow to compute the pedestrian pressure profile as a function of the distance to the wall. The profile is qualitatively similar to the one measured during an evacuation process. Fig. B.13 represents the histogram for the pressure on each pedestrian, computed as in Eq. 4 and Eq. A.2 (see caption for details).

[1] W. Cheng, S. Lo, Z. Fang, C. Cheng, A view on the means of fire prevention of ancient chinese buildings-from religious belief to practice, Structural Survey 22 (2004) 201209.

[2] OSHA, Design and construction requirements for exit routes, Occupational Safety & Health Administration Standards 29-CFR 1910.36(b) (2015) 1–3.

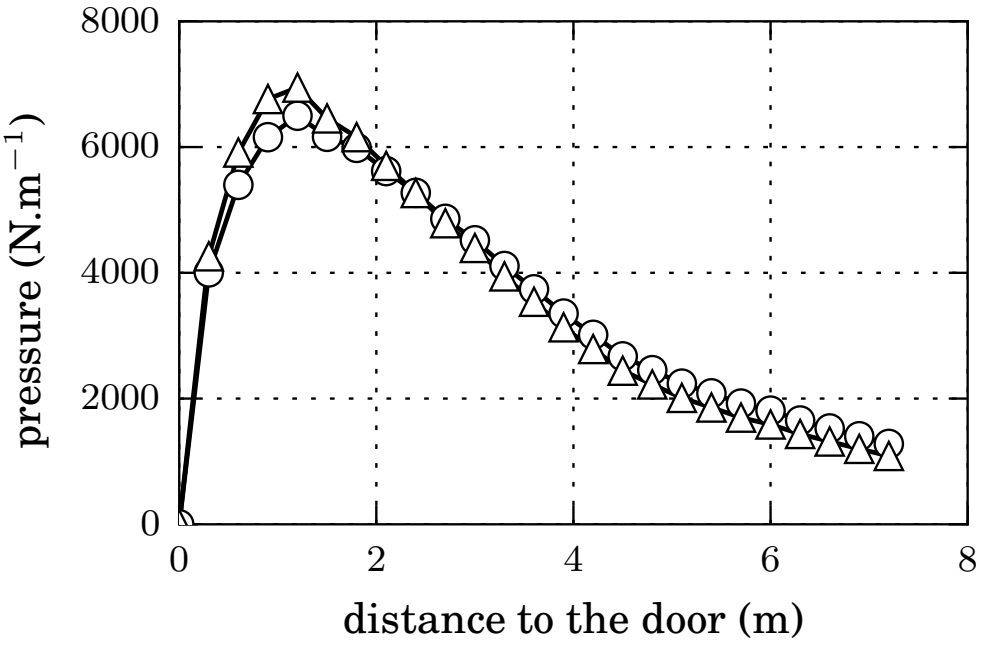

Figure B.13: Mean pressure as a function of the distance to the exit. The room was $20\,\mathrm{m} \times 20\,\mathrm{m}$ size and included one door of $d_w = 1.2$ m width. Mean values were computed from 30 evacuation processes, until 100 pedestrians left the room. The desired velocity was $v_d = 4\,\mathrm{m/s}$. The distance to the door was binned into equal intervals of 0.3 m. The $\bigcirc$ symbols correspond to the mean pressure computed as in A.2 for neglectable momentum ($p_i = 0$) and $\mathcal{A}_i = \pi r_i^2$. The symbols $\triangle$ correspond to the mean pressure computed as in 4 (see text for details).

[3] FBC2010, Exit and exit access doorways, Florida Building Code Handbook 1015.1 (2010) 90.

[4] FBC2010, Doors, gates and turnstiles, Florida Building Code Handbook 1008.1 (2010) 81.

[5] A. Kirchner, A. Schadschneider, Simulating of evacuation processes using a bionics-inspired cellular automaton model for pedestrian dynamics, Physica A 312 (2002) 260–276.

[6] G. Perez, G. Tapang, M. Lim, C. Saloma, Streaming, disruptive interference and power-law behavior in the exit dynamics of confined pedestrians, Physica A 312 (2002) 609–618.

[7] Z. Daoliang, Y. Lizhong, L. Jian, Exit dynamics of occupant evacuation in an emergency, Physica A 363 (2006) 501–511.

[8] T. Huan-Huan, D. Li-Yun, X. Yu, Influence of the exits' configuration on evacuation process in a room without obstacle, Physica A 420 (2015) 164–178.

[9] D. Parisi, C. Dorso, Microscopic dynamics of pedestrian evacuation, Physica A 354 (2005) 606–618.

[10] D. Helbing, I. Farkas, T. Vicsek, Simulating dynamical features of escape panic, Nature 407 (2000) 487–490.

[11] D. Parisi, C. Dorso, Morphological and dynamical aspects of the room evacuation process, Physica A 385 (2007) 343–355.

[12] G. Frank, C. Dorso, Room evacuation in the presence of an obstacle, Physica A 390 (2011) 2135–2145.

[13] G. Frank, C. Dorso, Evacuation under limited visibility, International Journal of Modern Physics C 26 (2015) 1–18.

[14] D. Helbing, P. Molnár, Social force model for pedestrian dynamics, Physical Review E 51 (1995) 4282–4286.

[15] M. Mysen, S. Berntsen, P. Nafstad, P. G. Schild, Occupancy density and benefits of demand-controlled ventilation in norwegian primary schools, Energy and Buildings 37 (12) (2005) 1234 – 1240.

693 doi:http://dx.doi.org/10.1016/j.enbuild.2005.01.003.
694 URL http://www.sciencedirect.com/science/article/pii/S037877880500040X

695 [16] S. Plimpton, Fast parallel algorithms for short-range molecular dy-
696 namics, Journal of Computational Physics 117 (1) (1995) 1 – 19.
697 doi:http://dx.doi.org/10.1006/jcph.1995.1039.
698 URL http://www.sciencedirect.com/science/article/pii/S002199918571039X

699 [17] X. Zhang, S. Zhang, G. Yang, P. Lin, Y. Tian, J. Wan, L. Yang, In-
700 vestigation of flow rate in a quasi-2d hopper with two symetric outlets,
701 Physics Letters A.

702 [18] J. Pastor, A. Garcimartin, P. Gago, J. Peralta, C. Gomez, L. Ferrer,
703 D. Maza, D. Parisi, L. Pugnaloni, I. Zuriguel, Experimental proof of
704 faster-is-slower in systems of frictional particles flowing through con-
705 strictions, Physical Review E.

706 [19] T. W. Lion, R. J. Allen, Computing the local pressure in molecular
707 dynamics simulations, Journal of Physics: Condensed Matter 24 (28)
708 (2012) 284133.
709 URL http://stacks.iop.org/0953-8984/24/i=28/a=284133